Depinning and creep in Josephson junction arrays in weak magnetic fields

Huan Liu,[1] Wei Zhou,[1] and Qing-Hu Chen[2,1,*]
[1]*Department of Physics, Zhejiang University, Hangzhou 310027, People's Republic of China*
[2]*CSTCMP and Department of Physics, Zhejiang Normal University, Jinhua 321004, People's Republic of China*
(Received 3 January 2008; revised manuscript received 7 July 2008; published 13 August 2008)

Based on resistively shunted junction dynamics, we have numerically studied the depinning transition and thermally activated creep motion of vortices in two-dimensional Josephson junction arrays exposed to a weak external field with the filling factor $f=1/25$. Whether the bond disorder is introduced into the system or not, a continuous depinning transition is found at zero temperature. By means of scaling analysis of the current-voltage characteristics, a non-Arrhenius creep law is observed at finite temperatures, with the existence of two universality classes depending on the strength of the bond disorder. The effects of the disorder on the critical current and critical exponents are also discussed.

DOI: 10.1103/PhysRevB.78.054509 PACS number(s): 74.25.Qt, 74.81.Fa, 75.40.Mg

I. INTRODUCTION

The dynamics of elastic systems is closely related to a variety of systems such as vortex lattices in type II superconductors,[1,2] charge-density waves in disordered systems,[3–5] Wigner crystals in a two-dimensional (2D) electron plasma,[6] domain walls in a magnetic film,[7] as well as driven interfaces in random media.[8] A fundamental challenge is how these systems respond to an external driving force, such as current-induced Lorentz force for vortices, electric field for charge-density waves, or magnetic field for domain walls. In the case of current-driven vortex systems, the competition between the repulsive vortex-vortex interaction and the attractive pinning potential produces many interesting dynamic properties, which have been explored extensively.[1,2,9–18] Recently, the depinning and creep motion of flux lines in three-dimensional (3D) systems have been investigated numerically based on overdamped London-Langevin model.[18]

Josephson junction arrays (JJAs) provide a well-controlled model for vortices moving in a periodic or random pinning environment in two dimensions. One can artificially modulate the coupling strength of the Josephson junctions as well as the external magnetic field. As we know, the discrete lattice structure induces an effective pinning potential which confines the motion of vortices. The complicated phase transitions of equilibrium and dynamic behaviors of this model have been studied considerably.[19–30] Theoretically, there have been some researches on the depinning and creep of vortices in 2D JJAs (Refs. 15 and 19–21); to the best of our knowledge, most of them were devoted to the depinning currents, and systematic studies on the nature of depinning transition and creeping motion are still lacking.

In this paper, based on resistively shunted junction (RSJ) dynamics, we will present a physical picture of depinning at zero temperature and creep at finite temperatures in 2D JJAs subjected to a weak external field with the magnetic-flux density $f=1/25$. Besides the critical current, the critical exponents are calculated, with the hope that these results can offer useful insights to further understand the behaviors of vortices. The rest of this paper is organized as follows. Section II describes the model and dynamic method. Section III shows our main results, where some discussions are also carried out. Finally, a short summary is given.

II. MODEL AND DYNAMIC METHOD

The Hamiltonian of 2D JJAs in an external magnetic field takes the following form:

$$H = -\sum_{\langle nm \rangle} J_{nm} \cos(\phi_n - \phi_m - A_{nm}), \tag{1}$$

where the induced magnetic field generated by currents is negligible, ϕ_n is the phase of the superconducting wave function on site n, the symbol $\Sigma_{\langle nm \rangle}$ denotes the summation over nearest neighbors m of n, J_{nm} is the strength of the Josephson coupling between nearest-neighboring sites, and $A_{nm} \equiv (2e/\hbar)\int_n^m \mathbf{A}\cdot d\mathbf{l}$ with $\mathbf{A}$ as the magnetic vector of a field $\mathbf{B}=\nabla\times\mathbf{A}$ perpendicular to the 2D JJAs. The summation of A_{nm} around any unit cell is $\Sigma_{\text{cell}} A_{nm}=2\pi f$, with $f=Ba^2/\phi_0$ (a is the array lattice constant and $\phi_0=h/2e$ is the magnetic-flux quantum) as the density of magnetic flux per unit cell. Just as mentioned above, f is chosen as $1/25$ in our simulations. The random pinning potential is introduced into the bond coupling strength $J_{nm}=J_0(1+p\varepsilon_{nm})$, where ε_{nm}'s are independently Gaussian distributed with zero mean and unit variance.[16,31] The well-known Kirkpatrick-Stoll random number generator is used for noise generation.[16] Here we focus on four values of p representing different levels of disorder: $p=0$, 0.05, 0.1, and 0.3. Note that in Ref. 23 for strongly disordered Josephson junction arrays, the value of strong disorder is equivalent to $p=1/4\sqrt{3}\approx 0.144$ in the present paper.

In our simulations, the RSJ dynamics is adopted, which can be written as[16]

$$\frac{\sigma\hbar}{2e}\sum_m (\dot{\phi}_n - \dot{\phi}_m) = -\frac{2e}{\hbar}\frac{\partial H}{\partial \phi_n} + I_n - \sum_m \Gamma_{nm}, \tag{2}$$

where I_n is the external current at site n which only exists at the boundary sites, Γ_{nm} is the thermal noise current with $\langle \Gamma_{nm}(t)\rangle = 0$, and $\langle \Gamma_{nm}(t)\Gamma_{kl}(0)\rangle = 2\sigma k_B T\delta(t)(\delta_{nk}\delta_{ml} - \delta_{nl}\delta_{mk})$, where the unit of temperature T is J_0/k_B. A uniform external current is injected into the system in the x direction. In order

to maintain the current[32] and ensure the periodic interactions between vortices,[33] the fluctuating twist boundary condition (FTBC) is used. Specifically, one introduces a global "twist" variable $\Delta_x(t)[\Delta_y(t)]$ to track the average phase drop per link in the $x(y)$ direction. Let $\theta_n \equiv \phi_n + \mathbf{r}_n \cdot \Delta$ be the excess phase at site n with $\Delta=(\Delta_x,\Delta_y)$ as the fluctuating twist variable. The gauge-invariant phase difference is replaced with $\Psi_{nm} = \theta_n - \theta_m - A_{nm} - (\mathbf{r}_n - \mathbf{r}_m)\cdot\Delta$, with θ_n as periodic in both x and y directions. To achieve a given current i through the sample, i.e., the sum of the normal current, the supercurrent, and the thermal noise current yields the desired total current, we require

$$\dot{\Delta}_x - \frac{1}{L^2}\sum_{\langle nm\rangle x}[(1+p\varepsilon_{nm})\sin(\Psi_{nm}) + \eta_{nm}] = i, \qquad (3)$$

where $\Sigma_{\langle nm\rangle x}$ denotes the summation over all links in the x direction. Equation (3) defines the dynamics of Δ_x.

The external current $i=I/I_{c0}$ and thermal noise current $\eta_{nm}=\Gamma_{nm}/I_{c0}$ are in units of $I_{c0}=2eJ_0/\hbar$. The unit of the time is $\sigma\hbar/2eI_{c0}$. The voltage exists only in the x direction $V=-L\dot{\Delta}_x$ in units of I_{c0}/σ. Obviously, the voltage relies on the system size L. Therefore, we measure the mean voltage per junction $v=V/L$. For convenience, units are taken as $2e=J_0=\hbar=\sigma=k_B=1$ in the following.

The above equations can be solved by a second-order Runge-Kutta method with time step $\Delta t=0.05$. The system size is $L=100$ over which the finite-size effect can be neglected. The results below are based on one realization of the disorder. For the present $L=100$ sample, a good self-averaging effect is expected. This is confirmed in a few additional simulations with different realizations of disorder, where the general results are not changed.

III. RESULTS AND DISCUSSIONS

In all simulations the ground-state phase configurations of the vortex system without disorder are selected as the initial state. To obtain the ground state, we begin to perform the simulations from high temperatures with random initial phase configurations and then gradually cool down the system to zero temperature. As a result, it is found that the ground state is a tilted squarelike vortex lattice, consistent with previous study.[21] In order to show the translational order of the vortex system, we calculate the vortex structure factor in the reciprocal space, which is defined as

$$S(\mathbf{k}) = \left|\frac{1}{L^2}\sum_j b(\mathbf{r}_j)\exp(z\mathbf{k}\cdot\mathbf{r}_j)\right|^2, \qquad (4)$$

where $b(\mathbf{r})$ is the vortex number through the unit cell at site $\mathbf{r}$ with $\Sigma_{\text{cell}}(\Psi_{nm})=2\pi[b(\mathbf{r})-f]$ and z is the unit imaginary number. As shown in panel (a) of Fig. 1 with brightness points, the vortex structure factor for $p=0$ at $T=0$ has periodic Bragg peaks, characteristic of the long-range order. In the presence of bond disorder, a ringlike pattern is observed in the structure factor for all disorders we studied. A structure factor for $p=0.1$ is exhibited in panel (b) of Fig. 1, indicating a disordered state. The vortex structure factors for $p=0.05$ and 0.3 (not shown here) are similar to that for $p=0.1$.

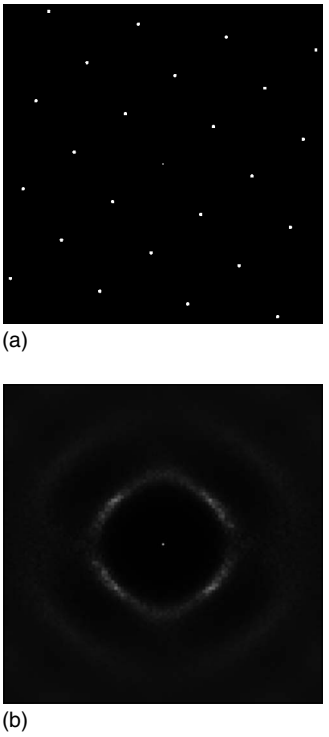

FIG. 1. Vortex structure factors at $T=0$ for $p=0$ (a) and $p=0.1$ (b) in a grayscale.

We proceed to the study of depinning transition. Figure 2 presents the $\log(v)$-$\log(i-i_{c0})$ curves at $T=0$ for all the p's considered. For each case, a continuous depinning transition is found, which can be described as $v\sim(i-i_{c0})^{\beta}$.[3,34] The corresponding critical currents i_{c0}'s and depinning exponents β's are estimated and illustrated in Fig. 2. Unexpectedly, the critical current varies nonmonotonously as the strength of the bond disorder builds up. The growing depinning exponent with the rise of disorder indicates that the dependence of the

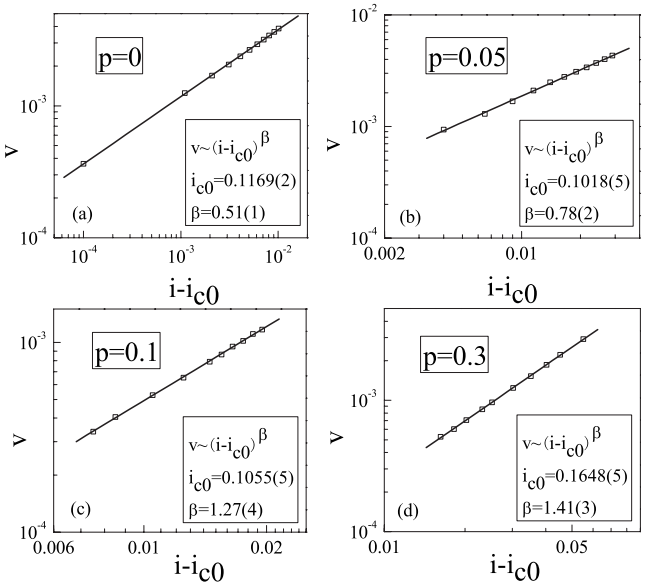

FIG. 2. $\text{Log}(v)$-$\log(i-i_{c0})$ plots at $T=0$ for (a) $p=0$, (b) $p=0.05$, (c) $p=0.1$, and (d) $p=0.3$. The real lines are fitting curves.

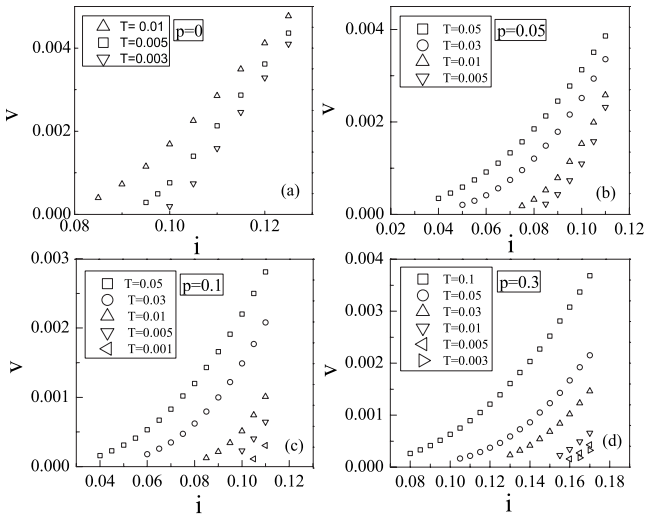

FIG. 3. v-i curves at finite temperatures for (a) $p=0$, (b) $p=0.05$, (c) $p=0.1$, and (d) $p=0.3$.

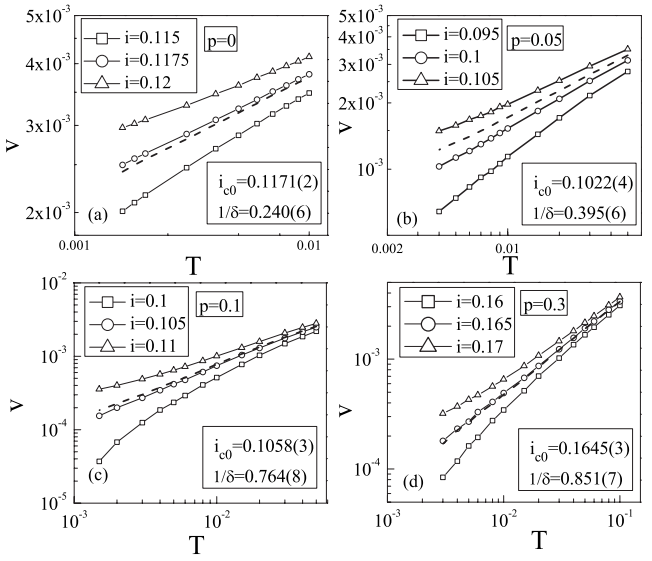

FIG. 4. Log-log plots of v-T at three currents around i_{c0} for (a) $p=0$, (b) $p=0.05$, (c) $p=0.1$, and (d) $p=0.3$. The dashed lines are at the critical currents. Lines are guides for the eyes.

voltage on the external driving current becomes stronger. Interestingly, in the pure system, the obtained $\beta=0.51(1)$ is in accord with that in the single-particle model within numerical errors,[3] which indicates that all vortices behave like an isolated vortex in the periodic potential.

Next, we discuss the creep motion of vortices at finite temperatures. As displayed in Fig. 3, the v-i curves for $T>0$ are rounded since the vortices may overcome the local energy barriers via the thermal activation energy. As expected, the creep motion speeds up with increasing temperature. To study the thermal rounding of the depinning transition quantitatively, in the mean-field theory Fisher[3] first predicted a scaling relation among the velocity, the driving force, and the temperature to analyze charge-density waves. Then the relation was successfully mapped into the random-field Ising model[35,36] and flux lines in type II superconductors.[18] In terms of the current-driven vortex systems, the dynamic scaling relation is cast into the following form:

$$v(T,i) = T^{1/\delta} G[T^{-1/\beta\delta}(i/i_{c0} - 1)], \tag{5}$$

with the scaling function $G(x \to 0)=$const. Namely, right at the critical current $i=i_{c0}$, the dependence of the voltage v on the temperature T scales as $v(T, i=i_{c0}) \sim T^{1/\delta}$ with the critical exponent $1/\delta$, which provides a method to determine the critical current i_{c0}.

The log-log v-T curves are plotted in Fig. 4 at three currents around i_{c0} for $p=0$, 0.05, 0.1, and 0.3. As we can see, the curves are concave for $i>i_{c0}$ and convex for $i<i_{c0}$ as the temperature decreases. It is expected that, only at $i=i_{c0}$, the v-T curve in a log-log scale exhibits the best power-law form. Similar to the process in Ref. 26, the critical current can also be evaluated by a quadratic interpolation method. The obtained i_{c0}'s are displayed in Fig. 4, consistent with those extracted from the depinning transition at $T=0$ within numerical errors. The temperature dependence of voltage at these critical currents is also shown in Fig. 4 with dashed lines. The slopes of these curves yield $1/\delta=0.240(6)$, 0.395(6), 0.764(8), and 0.851(7), which are also listed in Fig. 4. It is found that the critical exponent $1/\delta$ increases as the disorder goes up, indicating that the dependence of the voltage on the temperature at the critical current becomes stronger with the enhancement of disorder.

For each system studied, with δ and i_{c0} at hand, we carefully adjust the depinning exponent β until a very good collapse is achieved according to the scaling relation [Eq. (5)]. The scaling curves for four p's are presented in Fig. 5. The estimated values of β are 0.50(1), 0.79(2), 1.28(3), and 1.42(3), in agreement with those derived from the depinning transition within numerical errors. It is worth noting that the values of the combined exponent $\beta\delta=2.08(10)$, 2.00(5) for $p=0$ and 0.05 deviate from unity, as well as $\beta\delta=1.66(5)$,

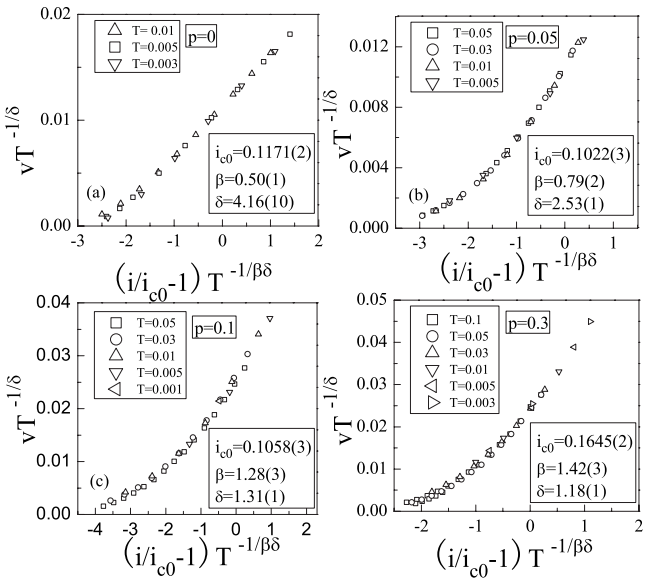

FIG. 5. Scaling curves of the data in Fig. 3 for (a) $p=0$, (b) $p=0.05$, (c) $p=0.1$, and (d) $p=0.3$.

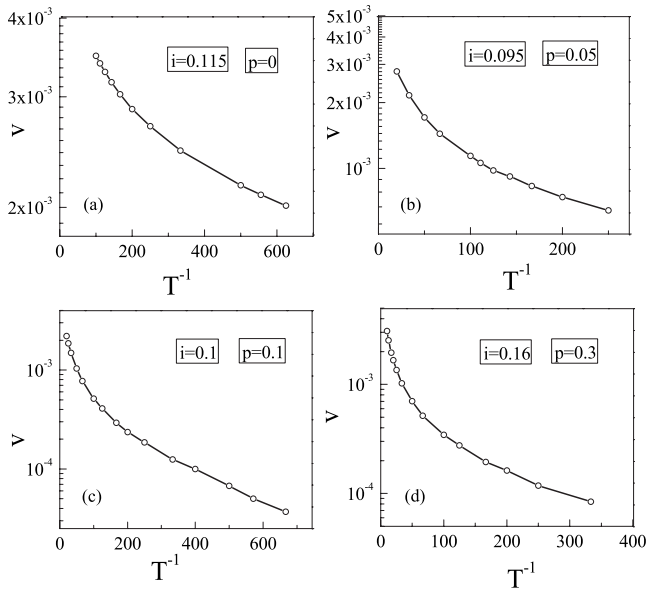

FIG. 6. Log(v) vs $1/T$ curves for (a) $p=0$, $i=0.115$, (b) $p=0.05$, $i=0.095$, (c) $p=0.1$, $i=0.1$, and (d) $p=0.3$, $i=0.16$. For each case, the current is smaller than the corresponding critical current. Lines are guides for the eyes.

1.68(5) for $p=0.1$ and 0.3. A well-known creep law is the Arrhenius type, in which the activation rate of vortices is proportional to $\exp[-U(i)/T]$, with $U(i)$ as the activation energy. However, all the scaling curves in Fig. 5 cannot be fitted by $\exp(-|x|^{\beta\delta})$ with each $\beta\delta$, illustrating that the creep laws are not the Arrhenius type. This non-Arrhenius-type creep can be confirmed in an alternative way. In Fig. 6, for each case, we plot log(v) vs $1/T$ curve at fixed current less than the corresponding critical current, a linear behavior is not observed, indicating really the absence of the Arrhenius behavior.

The non-Arrhenius-type creep behaviors have been previously observed in charge-density waves[5] and the flux lines in 3D systems with weak pinning;[18] however, the present exponents are different from previous ones. Interestingly, $\beta\delta$ is compatible with 2 for the $p=0$ and 0.05 and 5/3 for $p=0.1$ and 0.3 within standard deviations. The combination exponent $\beta\delta$ describes the temperature dependence of the creeping law, which is a crucial quantity in the scaling theory. Although the depinning exponent is dependent on the disorder strength, the combination exponent $\beta\delta$ has two different values from the weak to strong disorder, similar to the observation in Ref. 18. Since the selected four values of disorder represent different levels of disorder, these two characteristic values imply the existence of two universality classes in the 2D JJAs in a weak external magnetic field.

We also simulate the microscopic motions of vortices. At zero temperature, in the pure system once the external current exceeds the critical value, all vortices start to move simultaneously and follow the static channels when in motion. These channels become wider owing to thermal vibrations at finite temperatures. When the bond disorder is introduced, for currents slightly above the threshold value, some vortices move while others keep motionless and the channel disappears in this plastic motion. Since many dislocations are produced by the disorder, vortices move homogeneously. At finite temperatures, due to the thermal fluctuation, additional dislocations are induced in the creeping regime, yielding more homogeneous motion of vortices.

IV. CONCLUSIONS

We have studied the depinning and creep of vortices in the 2D JJAs with a dilute density of magnetic flux $f=1/25$. The results show that all these systems investigated exhibit a continuous depinning transition at zero temperature, while at finite temperatures, a non-Arrhenius creep law is found. The critical exponents β and $1/\delta$ increase as the bond disorder goes up. Furthermore, the product of two exponents $\beta\delta$ has two characteristic values, which suggest the existence of two universality classes depending on the strength of the bond disorder. Although a consistent picture of depinning and creep motion of vortices has been obtained numerically, the analytical theory for the nonlinear dynamic response in this system remains to be further developed. The experimental work on the depinning and creep in JJAs is called for to check the present numerical results.

ACKNOWLEDGMENTS

The authors acknowledge useful discussions with X. Hu and M. B. Luo. This work was supported by National Natural Science Foundation of China (Grant No. 10574107), PNCET and PCSIRT in University in China, and National Basic Research Program of China (Grant No. 2006CB601003).

*Corresponding author.

[1] G. Blatter, M. V. Feigel'man, V. B. Geshkenbein, A. I. Larkin, and V. M. Vinokur, Rev. Mod. Phys. **66**, 1125 (1994).
[2] M. Müller, D. A. Gorokhov, and G. Blatter, Phys. Rev. B **63**, 184305 (2001).
[3] D. S. Fisher, Phys. Rev. Lett. **50**, 1486 (1983); Phys. Rev. B **31**, 1396 (1985).
[4] G. Grüner, Rev. Mod. Phys. **60**, 1129 (1988).
[5] A. A. Middleton, Phys. Rev. B **45**, 9465 (1992).
[6] E. Y. Andrei, G. Deville, D. C. Glattli, F. I. B. Williams, E. Paris, and B. Etienne, Phys. Rev. Lett. **60**, 2765 (1988).
[7] S. Lemerle, J. Ferré, C. Chappert, V. Mathet, T. Giamarchi, and P. Le Doussal, Phys. Rev. Lett. **80**, 849 (1998).
[8] O. Narayan and D. S. Fisher, Phys. Rev. B **48**, 7030 (1993).
[9] S. Bhattacharya and M. J. Higgins, Phys. Rev. Lett. **70**, 2617 (1993).
[10] M. Marchevsky, J. Aarts, P. H. Kes, and M. V. Indenbom, Phys. Rev. Lett. **78**, 531 (1997).
[11] A. E. Koshelev and V. M. Vinokur, Phys. Rev. Lett. **73**, 3580 (1994).

[12] T. Giamarchi and P. Le Doussal, Phys. Rev. Lett. **76**, 3408 (1996); **78**, 752 (1997); P. Le Doussal and T. Giamarchi, Phys. Rev. B **57**, 11356 (1998).
[13] L. Balents, M. C. Marchetti, and L. Radzihovsky, Phys. Rev. Lett. **78**, 751 (1997); Phys. Rev. B **57**, 7705 (1998).
[14] S. Scheidl and V. M. Vinokur, Phys. Rev. B **57**, 13800 (1998).
[15] S. Brazovskii and T. Nattermann, Adv. Phys. **53**, 177 (2004).
[16] Q. H. Chen and X. Hu, Phys. Rev. Lett. **90**, 117005 (2003).
[17] Q. H. Chen and X. Hu, Phys. Rev. B **75**, 064504 (2007).
[18] M. B. Luo and X. Hu, Phys. Rev. Lett. **98**, 267002 (2007).
[19] J. S. Chung, K. H. Lee, and D. Stroud, Phys. Rev. B **40**, 6570 (1989).
[20] D. Domínguez, Phys. Rev. Lett. **72**, 3096 (1994).
[21] V. I. Marconi and D. Domínguez, Phys. Rev. Lett. **82**, 4922 (1999); Phys. Rev. B **63**, 174509 (2001).
[22] W. Yu, K. H. Lee, and D. Stroud, Phys. Rev. B **47**, 5906 (1993).
[23] D. Domínguez, Phys. Rev. Lett. **82**, 181 (1999).
[24] K. D. Fisher, D. Stroud, and L. Janin, Phys. Rev. B **60**, 15371 (1999).
[25] Q. H. Chen, M. B. Luo, and Zh. K. Jiao, Phys. Rev. B **64**, 212403 (2001).
[26] Q. M. Nie, M. B. Luo, and Q. H. Chen, Phys. Rev. B **74**, 024523 (2006).
[27] M. Franz and S. Teitel, Phys. Rev. Lett. **73**, 480 (1994).
[28] M. B. Luo and Q. H. Chen, Eur. Phys. J. B **35**, 201 (2003).
[29] A.-L. Eichenberger, J. Affolter, M. Willemin, M. Mombelli, H. Beck, P. Martinoli, and S. E. Korshunov, Phys. Rev. Lett. **77**, 3905 (1996).
[30] E. Granato and D. Domínguez, Phys. Rev. B **56**, 14671 (1997).
[31] P. Olsson and S. Teitel, Phys. Rev. Lett. **87**, 137001 (2001).
[32] B. J. Kim, P. Minnhagen, and P. Olsson, Phys. Rev. B **59**, 11506 (1999).
[33] P. Olsson, Phys. Rev. B **46**, 14598 (1992); **52**, 4511 (1995); **52**, 4526 (1995).
[34] P. Chauve, T. Giamarchi, and P. Le Doussal, Phys. Rev. B **62**, 6241 (2000).
[35] U. Nowak and K. D. Usadel, Europhys. Lett. **44**, 634 (1998).
[36] L. Roters, A. Hucht, S. Lübeck, U. Nowak, and K. D. Usadel, Phys. Rev. E **60**, 5202 (1999).